Extrusion Foaming of Poly(styrene-*co*-acrylonitrile)/Clay Nanocomposites Using Supercritical CO_2[a]

Laetitia Urbanczyk, Michaël Alexandre, Christophe Detrembleur, Christine Jérôme,* Cédric Calberg

Supercritical CO_2 has been used as a blowing agent to foam poly(styrene-*co*-acrylonitrile)-based materials in a single screw extruder specially adapted to allow fluid injection. The cellular morphology depends on foaming temperature, more regular cells being obtained with decreasing extrusion temperature. In a second step, a natural and an organomodified nanoclay have been added for the purpose of imparting some flame resistance to the foamed material. The filler efficiency in reducing sample combustion rate appeared to be dependent on its delamination level inside the matrix and better results were obtained when the organomodified clay was first delaminated in the polymer in an efficient twin screw extruder using water assistance, prior to foaming in the single screw extruder.

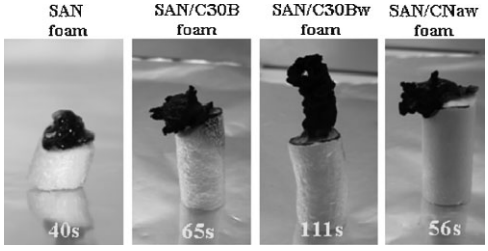

Introduction

Polymeric foams are cellular materials with wide applications in insulating, packaging and automotive industry because of their low weight, high strength-to-weight ratio, good insulating properties and high impact strength.[1–3] Furthermore, the steady increase of oil prices in recent years has led to an increase of plastic costs. Producing plastic foams can thus be an alternative to decrease the amount of resin used, as long as foams keep acceptable mechanical properties.[4] In this context, microcellular foams with controlled cell morphology are very attractive because they exhibit better impact resistance over conventional plastic foams having larger cells.[5–6] It is also noteworthy that foam stiffness is directly related to foam density and cell regularity.[7] While traditional foaming processes have mainly relied on hydrocarbons or fluorocarbons (CFCs) as physical blowing agents, efforts are now devoted to use more environmentally friendly gases.[2]

In this study, we have used supercritical (sc) CO_2 as physical blowing agent in a specially designed single-screw extruder. This fluid was chosen for several reasons: it is cheap, non-toxic, inert, non-flammable, environmentally friendly compared to CFCs and it has easily attainable sc conditions (31.1 °C, 73.8 bar). Moreover, CO_2 under sc conditions can be dissolved into a large panel of polymer matrices to form a single-phase polymer/fluid solution.[8–9] The melt viscosity is highly decreased during this step, due

L. Urbanczyk, M. Alexandre, C. Detrembleur, C. Jérôme
Center for Education and Research on Macromolecules (CERM), University of Liege, Building B6, 4000 Liège, Belgium
Fax: +32 4 366 3497; E-mail: c.jerome@ulg.ac.be
C. Calberg
Department of Applied Chemistry, University of Liege, Building B6, 4000 Liège, Belgium

[a] Supporting information for this article is available at the bottom of the article's abstract page, which can be accessed from the journal's homepage at http://www.mme-journal.de, or from the author.

DOI: 10.1002/mame.201000078

to the plasticization effect of the fluid,[8] as shown in a previous work.[10] When the polymer/CO_2 solution reaches the die, a sudden pressure drop occurs. This induces sudden phase demixing, which takes place by generating a large quantity of bubbles in the polymer (nucleation).[11] Cell growth then occurs until the foam is frozen (when $T < T_g$).[12]

Polymeric foams are used in a large panel of applications in isolation, house decoration, etc. For those kinds of proximity applications, the material should meet some fire safety requirements. Brominated or chlorinated fire retardants are most of the time added to fireproof the material.[13] Nowadays, the research focuses on halogen-free flame retardants due to environmental and health concerns.[14–15] In that context, nanoclays are attracting an increasing interest due to their well-known flame retardant effect at very low level (3–5 wt.-%).[16–18] In opposition with usual flame retardants, nanoclays may also mechanically reinforce foams, thus enhancing both properties at once, which is unique. Their flame retardant efficiency has already been demonstrated in some polymeric foams like polyurethane,[19–20] polystyrene (PS)[21] or poly(styrene-*co*-acrylonitrile) (SAN).[22] Nanoclays combined with classical flame retardants can also act in synergy to reduce flammability, as already shown in plain[23–24] or foamed materials.[22]

Extrusion foaming of polymer/clay nanocomposites has already been described in the literature with various polymers like PS,[21] polyamide 6,[25] low-density polyethylene[26] and PS/poly(methyl methacrylate) blend.[27] As a general trend, nanocomposite foams have smaller cell size and higher cell density compared to the unfilled polymeric foam, while the increased melt strength reduces cell coalescence phenomenon. This kind of nanocomposite foam has also improved fire behavior or mechanical properties, as demonstrated by Han et al.[21]

The present study reports on the continuous production of SAN foams with sc carbon dioxide as foaming agent in a home-designed single-screw extruder, which has never been described in the literature yet. Attention has been paid to the influence of the temperature profile in the extruder on cell morphology and foam density. Foam cooling at the exit of the extrusion line has also been envisaged as it was known that this treatment improves the foam morphology by freezing the foam earlier, in order to limit cell coalescence.[11,12,28] Then, the influence of nanoclays on the foam morphology has been investigated as a function of their de-aggregation degree inside the polymer. For that purpose, the clay has either been directly added in the feeder with the polymer (one-pot), or it has first been dispersed in the polymer in an efficient twin-screw extruder before being foamed in the $scCO_2$ extruder (two-step). The fire behavior of the prepared nanocomposite foams was finally evaluated qualitatively and with limiting oxygen index (LOI) test.

Experimental Part

Materials

SAN with an acrylonitrile content of 25 wt.-% (Luran® 358N, BASF) was used in these experiments. CO_2, used as foaming agent, was provided by Air Liquide (99.995%). Cloisite® Na^+ (CNa) and Cloisite® 30B (C30B) are lamellar montmorillonite clays from Southern Clay Products (Texas, USA). The first one is a natural clay while the second one is organomodified with bis[2-(hydroxyethyl)methyl]tallowalkylammonium cations. Home-made pre-exfoliated organoclay, MB30B, was also used in this study. This filler contains 53 wt.-% of inorganic clay, 13 wt.-% of the same ammonium as C30B and 34 wt.-% of poly(ε-caprolactone) chains mainly grown from the ammonium hydroxyl groups. The preparation of this highly filled pre-exfoliated clay, also called masterbatch, was undergone in sc CO_2 in order to take advantage of this unusual polymerization medium. All the details about its synthesis and characterization can be found in ref. [29]

Setup

A schematic diagram of the experimental equipment used for continuous polymer foaming with $scCO_2$ is shown in Figure 1. Basically, it consists of a single-screw extruder from Brabender® (19/25D) coupled with a gear pump. A multi-stage screw with one feed section, two compression sections and one mixing section was especially designed for this kind of application. The polymer was introduced through the hopper and melted in the first compression section of the screw. Carbon dioxide was compressed with a syringe pump (ISCO 260D) and injected into the mixing zone at a constant volumetric flow. In order to improve the gas dispersion inside the polymer, a high pressure melt pump and a static mixer were fixed at the end of the extruder barrel to increase the pressure and the residence time of the matter inside the equipment, respectively. The filamentary die is cylindrical and its length can be adjusted with a screw to control the magnitude of the pressure drop.[30]

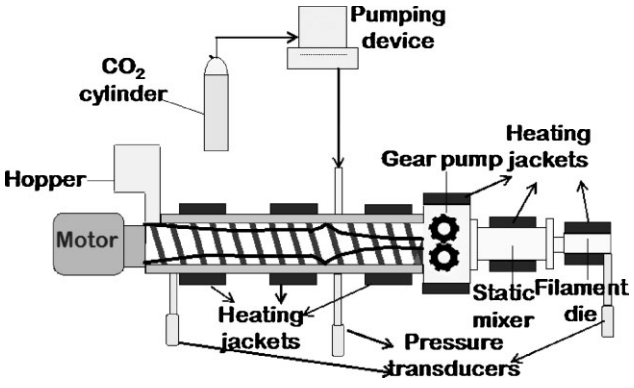

Figure 1. Experimental setup used for the continuous production of SAN microcellular foams.

Macromol. Mater. Eng. **2010**, *295*, 915–922

Macromolecular Journals
DOI: 10.1002/mame.201000078

Procedure

SAN pellets were added alone or in combination with nanoclay (C30B or MB30B) in the feed. Then, the polymer was melted at 190 °C in the first compression section of the screw. Polymer/clay nanocomposite pellets, obtained from water-assisted twin-screw extrusion (SAN/CNaw, SAN/C30Bw), were added in the same way than neat polymer. The details about nanocomposite extrusion in this extruder can be found in ref. [31] The inorganic content was set at 3 wt.-% for all nanocomposite foams. Carbon dioxide was injected at 150 bar at a constant volumetric flow rate of $0.5\,mL \cdot min^{-1}$. After a short period of time, the operating temperature of all the heating jackets placed after the gas injection was gradually decreased, in order to increase the viscosity of the polymer/CO_2 solution. The pressure at the die exit was always adjusted to 300 bar. The produced foams were cooled under ambient conditions or actively cooled by air flushing at the die exit to freeze foams earlier during their expansion.

Characterization Techniques

X-ray diffraction (XRD) was carried out with a powder diffractometer Siemens D5000 (Cu K_α radiation with $\lambda = 0.15406$ nm, 50 kV, 40 mA, Ni filter, $\theta/2\theta$ geometry) at room temperature for 2θ varying from 1.65 to 30° in steps of 0.04°, in order to characterize the final morphology of nonfoamed composites.

Nanoclay distribution in SAN was directly observed by transmission electron microscopy (TEM, Philips CM100). Ultrathin sections (50–80 nm) were prepared with an ultramicrotome Ultracut FC4e, Reichert-Jung. No staining was used since the alumosilicate sheets are contrasting enough in the polymer matrix.

Foam density was calculated by measuring the sample weight and volume. The cell structure was examined by scanning electron microscopy (SEM) with a JEOL JSM 840-A apparatus. The fractured surface was metalized with Pt (30 nm) before observation. The LOI test was performed in order to assess fire behavior of the foams, with a limiting oxygen indexer from Fire Instrumentation and Research Equipment Ltd. The aim was to measure the minimum oxygen concentration necessary to support a candle-like combustion of materials. Foamed samples of cylindrical shape directly obtained upon foam extrusion were tested. Measurements were performed three times and average value is reported. The precision on LOI value lies around 1 vol.-%.

Results and Discussion

Neat SAN Foams

Effect of Die Temperature

We investigated the influence of two experimental parameters on SAN foams morphology. First, the temperature of the polymer/CO_2 solution has been gradually decreased from 180 °C down to a minimum value of 143 °C in the die, the high pressure melt pump and the static mixer. Below this temperature, the melt viscosity became too high and the torque of the pump exceeded its maximum value. Under the selected experimental conditions, 5 wt.-% of CO_2 was dissolved into SAN. The foams morphology analyzed by SEM as a function of temperature is presented in Figure 2, whereas pictures of the samples produced under the same conditions but directly cooled by air flushing at the die exit can be found in Figure S1 (Supporting Information).

SAN foam produced at high temperature (180 °C) is very irregular with undefined cell morphology (Figure 2a). Pores seem to have collapsed during foaming. This phenomenon was well described by Park and co-workers.[12,32] Indeed, at such a high temperature, cells have more time to grow, leading to thinner cell walls. This favors gas diffusion out of the cells through the very thin cell walls. As a result, the pressure inside the cells is reduced, and this leads to foam contraction. This phenomenon is visually observable by

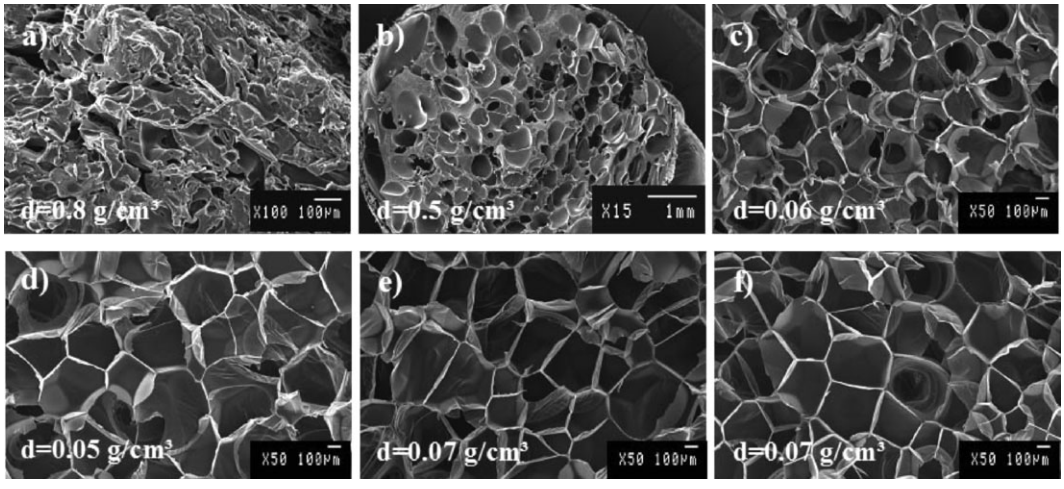

Figure 2. SEM analysis of SAN foams produced at various extrusion temperatures, without cooling at the end of the extrusion line: (a) 180, (b) 170, (c) 160, (d) 150, (e) 145 and (f) 143 °C.

looking at the foam diameter during the continuous extrusion: the foam first expands and then shrinks rapidly, leading to a poorly foamed sample with a rough skin, which is consistent with the gas escape explanation. Cell collapse also occurs due to the too low melt strength which cannot withstand such porous structure (Figure 2a). The density of this foam is very high (0.8 $g \cdot cm^{-3}$, see Figure 3), since the majority of the cells have collapsed.

When the temperature was decreased to 170 °C (Figure 2b), pores became more regular as a result of the increase of the melt strength. The cell collapse is thus limited. However, part of the CO_2 still diffuses out of the porous structures as indicated by the rough aspect of the foam skin. This explains the quite high density – 0.5 $g \cdot cm^{-3}$ – of this foam. Some cells are very large (up to 0.8 mm in diameter), due to cell coalescence occurring after a too long cell growth time.

The foam produced at 160 °C (Figure 2c) is characterized by regular pores that are mostly connected to each other, giving rise to an essentially open porosity. This means that the viscosity of the melt solution is still not high enough to prevent cell coalescence. The average cell diameter lies around a few hundreds of micrometers. The large decrease of the foam density down to 0.06 $g \cdot cm^{-3}$ proves that the majority of the injected CO_2 was used for foam expansion and that gas loss through the foam skin was prevented under these conditions (smooth skin).

When decreasing the temperature to 150 °C, a well defined porous structure was obtained and no more cell coalescence was detected in the SEM pictures (Figure 2d). The cell size ranges from 100 to 300 μm and the foam density falls to 0.05 $g \cdot cm^{-3}$ – the lowest value we reached for SAN. Indeed, a further decrease of temperature to 145 or 143 °C (Figure 2e and f, respectively) leads to slightly higher foam densities of 0.07 $g \cdot cm^{-3}$, with similar foam morphology. This can be explained by a quick freeze of the foam which stops the cell growth. We can estimate the critical volume expansion ratio, $Vf/V0$, for the SAN/ CO_2 system, with 5 wt.-% of gas, considering that 100% of the gas is used for foam expansion:[32]

$$\frac{Vf}{V0} = \frac{(\text{polymer volume} + \text{gas volume})}{\text{polymer volume}} \quad (1)$$

$$= 1 + \frac{m_{CO_2}}{m_{SAN}} \cdot \frac{\rho_{SAN}}{\rho_{CO_2}} \quad (2)$$

$$= 1 + 0.05x\left(\frac{1.08}{0.0018}\right) \cong 31 \quad (3)$$

where ρ_{SAN} and ρ_{CO_2} are SAN and CO_2 density at room temperature, and equal 0.0018[32] and 1.08[33], respectively. The theoretical maximum expansion ratio calculated is about 31, but in these experiments, we only achieved a maximum of 20-fold increase in SAN volume ($d = 0.05\ g \cdot cm^{-3}$). This means that part of the CO_2 is not used for expanding foams.

We can conclude that SAN foams with a regular morphology were obtained when the temperature of the polymer/CO_2 solution was chosen between 150 and 143 °C. Under these conditions, the polymer melt strength prevents gas loss and cell coalescence during foam expansion.

Effect of Air Cooling

The same experiments were performed with applying an air flush on the surface of the extruded foams at the nozzle exit in order to limit gas escape from the foam skin and to get rid of foam shrinking after its expansion. An improvement was thus expected at higher melt temperature, where gas loss was obvious. In this context, the effect of air cooling on foam density and cell morphology was studied in the whole investigated temperature range. A striking influence was observed at 180 and 170 °C, as the foam expansion ratio was approximately doubled (Figure 3). Freezing the foam skin thus allowed the cell growth inside the cylindrical samples. However, only the external part of the foam was cooled down and no beneficial effect was observed on cellular morphology, as cell coalescence still predominated (Figure S1a).

Down 170 °C, the influence of air cooling on cell morphology was less obvious as a similar density was observed with or without air flush at a same nozzle temperature (Figure S1b).

As seen in Figure 3, in the 143–150 °C range, foam densities were slightly higher under than without cooling. This may be explained by a restricted cell growth due to a faster foam freezing. This set of experiments thus shows the huge importance of homogenizing the temperature profile in the extrudate for preparing regular and well-expanded foams.

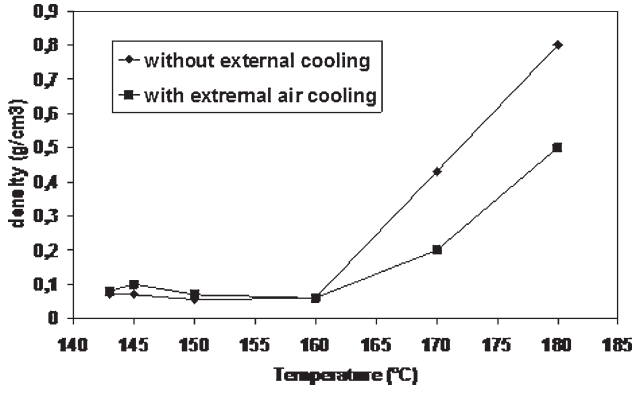

Figure 3. Density of SAN foams versus die temperature, without (◆) and with external cooling (■).

Macromolecular Journals
DOI: 10.1002/mame.201000078

SAN/Clay Nanocomposite Foams

Nanocomposite foams were first prepared in a one pot process, where the clay and the polymer pellets were introduced together in the feeder. An accurate amount of filler was added in order to reach a final inorganic content of 3 wt.-% in the material. Foams obtained in the 160–150 °C temperature range have similar expansion ratios and cell sizes compared to neat SAN foams (Figure 4). However, some bigger voids of ≈1 mm are observable in the SEM pictures (arrows). These defects may result from residual clay stacks not fully dispersed in the polymer.

This assumption was checked by extruding filler/polymer mixtures without gas injection. For example, samples containing 3 wt.-% of C30B (SAN/C30B) were cloudy and full of big clay stacks easily discernible (Figure S2a). The masterbatch MB30B, which already showed very nice dispersion into SAN when batch-mixed in an internal mixer,[34] was also dispersed into SAN in the extruder. The material obtained (SAN/MB30B) is translucent but it also contains some non-dispersed clay aggregates (Figure S2b). Nevertheless, an increase of the interlayer distance has been evidenced in both cases with XRD analysis (Figure S3). This reveals that the polymer managed to penetrate between the clay platelets. The polymer has thus a good affinity for the clay, but the shear applied by the single screw is not sufficient to break all the clay stacks and to fully delaminate the clay at the sub-μm level.

In order to enhance the nanoclay dispersion level, the envisaged strategy consists in first dispersing the nanofiller into SAN in an efficient twin screw extruder, and then to foam this nanocomposite in the single screw extruder coupled with CO_2 injection. Nanoclay dispersion was performed in a semi-industrial scale twin screw extruder specially designed to allow water injection during extrusion.[35] Water was removed at the end of the extrusion process under vacuum, leading to dry nanocomposites. We had recently highlighted the beneficial effect of water injected on CNa^+ and C30B delamination into SAN during extrusion.[31] Water clearly helps clay de-aggregation into SAN, leading to perfectly transparent samples with both commercial clays (Figure S2c–d). However, water did not promote polymer intercalation into natural clay. In fact, the XRD signal of Cloisite® Na^+ remained unaffected after water-assisted extrusion (SAN/CNaw, Table 1 and Figure S3b). In contrast, the nanocomposite based on C30B extruded with water (SAN/C30Bw) contains a large portion of exfoliated platelets, in co-existence with some residual small stacks as testified by XRD and transmission electron microscopy (TEM) analyses (Figure S3a and Figure 5). In fact, the clay platelets in SAN/C30Bw are well separated from each other (Figure 5a), whereas the filler in SAN/CNaw remains aggregated in small stacks homogeneously distributed in the matrix (Figure 5b and c). Water injected during extrusion thus weakens physical bonds responsible for clay natural aggregation and favors break-up of these

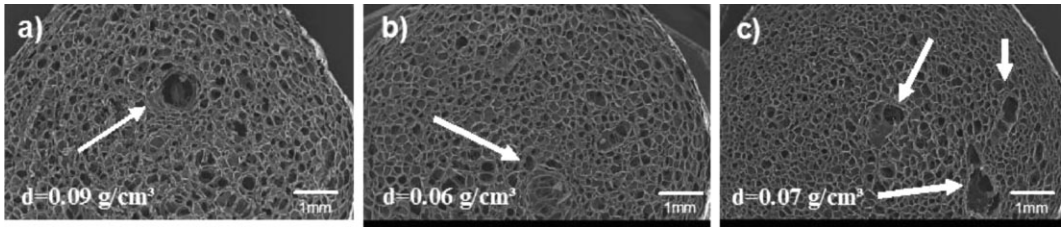

Figure 4. SEM analysis of SAN foams containing 3 wt.-% of C30B prepared in one pot in the extruder with CO_2 at different nozzle temperatures: (a) 160, (b) 155, and (c) 150 °C. Arrows show some foam defects.

Table 1. Extrusion conditions of SAN/clay nanocomposites at 175 °C without CO_2 injection.

Sample	Extruder type	Torque	Interlayer distance	Visual inspection
		N	nm	
SAN	single-screw	40	no signal	translucent
SAN/C30B		85	3.6	cloudy + visible clay stacks
SAN/MB30B		30	3.6	translucent + visible clay stacks
SAN/CNaw	twin-screw with water injection	60	1.1	translucent
SAN/C30Bw		80	no signal	translucent

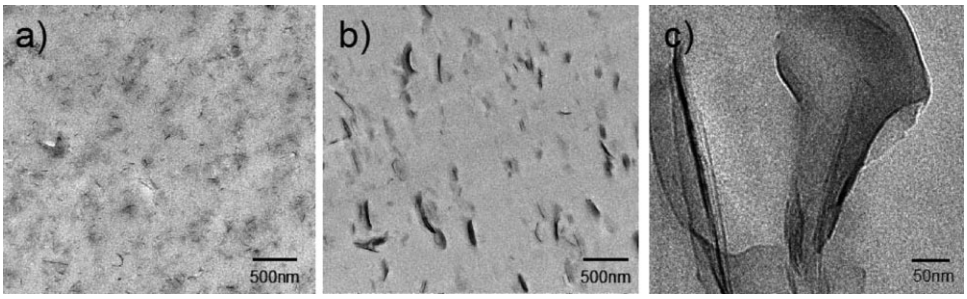

Figure 5. TEM pictures of (a) SAN/C30Bw and (b–c) SAN/CNaw nanocomposites prepared in a twin screw extruder using water injection.[31]

big stacks. However, even if CNa^+ is swelled by water, polymer intercalation in the natural clay seems not thermodynamically favored with slightly polar polymers like SAN. This behavior contrasts with the results reported in another work,[35] where the natural clay was fully exfoliated in a polar polymer, polyamide 6, thanks to water-assisted extrusion.

Those two nanocomposites were pelletized and then introduced in the single screw extruder for the foaming step. The foaming conditions are detailed in Table 2. The nozzle temperature was progressively decreased until the lowest reachable value, under which the viscosity becomes too high for the extruder to maintain the requested melt flow rate. 143 °C was the lowest temperature reachable for pure SAN and it increased to 152 °C for SAN/CNaw and to 160 °C for SAN/C30Bw. This trend is consistent with the increased viscosity upon nanoclay addition, the effect being more important for the largely exfoliated clay.[36]

The density of the produced foams decreased with the nozzle temperature (Table 2). This phenomenon is consistent with a higher amount of CO_2 retained in the sample at low temperature. However, at too low temperature (152 °C for SAN/CNaw), foam expansion was restricted due to the rapid sample freezing, which prevented the foam to reach its maximum expansion ratio.

SEM analysis shows very regular cells below 170 °C devoid of defects, in contrast with those prepared with the 'one step' process (Figure 6 and 7). These results support the assumption previously made on clay stacks being the source of these big voids in the foam.

A partially open cellular porosity is observed for both nanocomposite foams, with cell sizes of 200–300 μm for SAN/C30Bw and 100–200 μm for SAN/CNaw. The smaller

Table 2. Extrusion foaming conditions of nanocomposites previously prepared in the twin screw extruder and corresponding foam densities.

Nanocomposite	Nozzle *T*°	Torque	Density
	°C	N	$g \cdot cm^{-3}$
SAN/C30Bw	170	49	0.13
	165	55	0.09
	163	53	0.085
	160	55	0.08
SAN/CNaw	170	48	0.20
	160		0.085
	155		0.075
	152		0.09

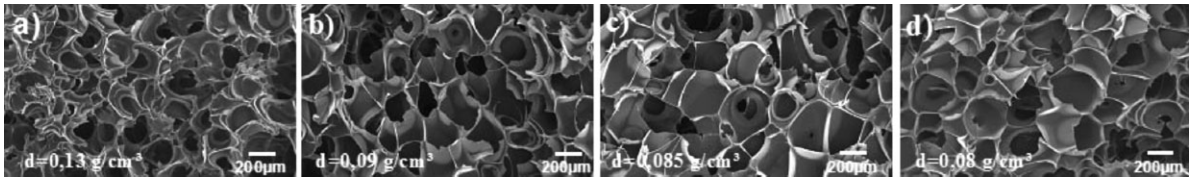

Figure 6. SEM analysis of SAN/C30Bw foams prepared at different extrusion temperatures: (a) 170, (b) 165, (c) 163, and (d) 160 °C.

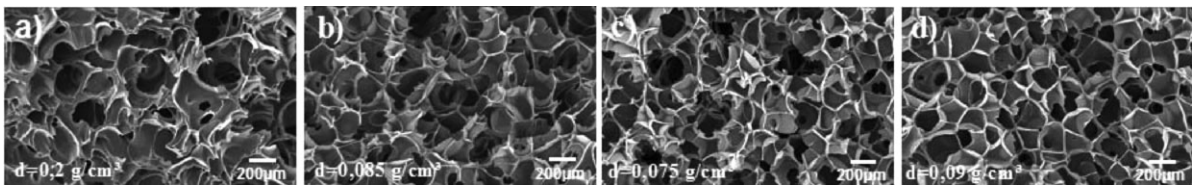

Figure 7. SEM analysis of SAN/CNaw foams prepared at different extrusion temperatures: (a) 170, (b) 160, (c) 155, and (d) 152 °C.

Macromol. Mater. Eng. **2010**, *295*, 915–922

Macromolecular Journals
DOI: 10.1002/mame.201000078

cell size observed in the latter composite foam might be related to cells nucleated at the surface of finely dispersed CNa particles.[21]

Extruding first the nanocomposite in a twin screw extruder thus allowed preparing nanocomposite foams with regular cellular structure in a continuous way with a single screw extruder using CO_2 as the blowing agent. Optimizing the foaming temperature led to highly expanded foams.

Fire Behavior

All the nanocomposite foams prepared in this work were subjected to a small flame (lighter) for 5 s in vertical orientation in order to observe their burning behavior in a qualitative way (Figure 8). Pure SAN foam burned fast (40 s) and produced burning drips, whereas nanocomposite foams burned more slowly (56–111 s) without dripping. A carbonaceous char was formed upon combustion of nanoclay-filled foams.[22] This layer contributed to reduce the fire propagation rate by both physically protecting the polymer from the flame and by slowing down the diffusion of the volatile degradation products towards the flame.[18] The fire retardant efficiency of this kind of nanocomposite is directly related to the cohesiveness of such char. In our case, it is amazing to see that a resistant and cohesive char can be formed in the case of largely exfoliated nanocomposite foam (SAN/C30Bw, Figure 8c), despite the fact that this material contains 90% of voids. This sample has the slowest burning rate, which confirms the improved flame resistance of this material. It must be mentioned that none of these samples self-extinguished during this test.

Following this qualitative test, we can affirm that nanoclay delamination at the nanometric level inside the polymer is a critical step to achieve efficient flame retardant behavior.

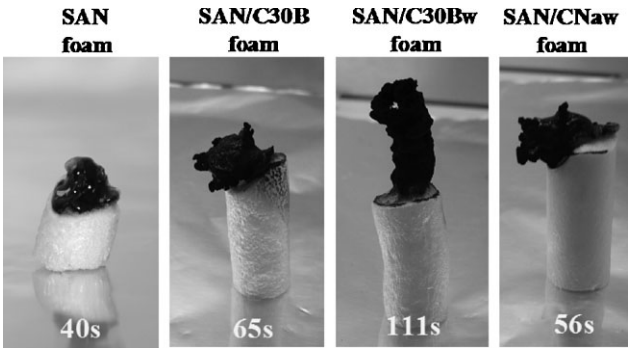

Figure 8. Fire test of SAN and SAN/clay nanocomposite foams prepared in the extruder ($d = 0.1\,g \cdot cm^{-3}$). The time needed for 5 cm of the foam to burn has been measured.

An oxygen index test was performed in order to determine the LOI of the material and therefore, quantify its fire resistance. This test allowed the determination of the lowest oxygen concentration needed to maintain regular burning of the sample.

A high LOI value means that the material has low flammability. Pure SAN foam exhibited a LOI of 19.6 vol.-%. This value was unchanged for the foam containing intercalated C30B (19.5 vol.-%) and it increased to 20.5 vol.-% for the exfoliated nanocomposite foam (C30Bw). However, this jump remains within the experimental error (1 vol.-%) and we thus cannot affirm on the basis of those results that nanoclay really affects the LOI of SAN foam. Similar results were reported in the literature concerning plain nanocomposites, where LOI was not influenced by this kind of nanofiller, despite of their gas barrier property.[24,37] In contrast to those nanofillers, which only act in the solid phase, other flame retardants, which are active in the gas phase, can increase the LOI of polymers up to 25 or 30 vol.-%, providing a sufficient amount of additive is introduced (usually 10–50 wt.-%).[18,38–39]

Conclusion

Low-density SAN foams have been successfully produced in a continuous process using $scCO_2$ as a foaming agent. The effect of a progressive decrease of the working temperature on foam morphology has been studied, from 180 to 143 °C. At high temperature, the produced foams are characterized by a high density since foam shrinkage could not be avoided. The decrease of the processing temperature progressively suppresses the gas diffusion out of the cells as well as the cell coalescence thanks to a higher melt viscosity. SAN foams with regular porosity have been obtained in the 150–143 °C temperature range. Cooling the extruded foam at the exit of the nozzle with an air flush allows preparing foams with low densities but was notable to prevent cell coalescence during foam expansion.

Adding commercial or pre-exfoliated nanoclays together with the polymer in the foaming extrusion process leads to regular foams when nanofillers were well dispersed in the polymer mixture. Foams with well-defined cell size and morphology have thus been prepared thanks to a two-stage process, where an 'ideal' filler dispersion is first achieved in a twin-screw extruder using water injection.

The burning behavior of these foams is significantly enhanced compared to neat SAN foam. In fact, melt dripping is prevented and burning time is increased due to the nanoclay flame retarding ability. The best result is obtained for the nanocomposite exhibiting an exfoliated morphology, thanks to the protective carbonaceous char formed during combustion.

Acknowledgements: CERM is grateful for the financial support from the '*Interuniversity Attraction Poles*' Programme PAI P6/27 – Belgian State – *Belgian Science Policy* and from the '*Région Wallonne*' in the frame of the WINNOMAT program: PROCOMO. C. D. is "Senior Research Associate" by *F.R.S. – FNRS*, Belgium. The authors thank Dr *S. Benali* and Prof. *P. Dubois* (SMPC, UMons, Mons, Belgium) for LOI tests.

Received: March 1, 2010; Revised: May 19, 2010; Published online: August 31, 2010; DOI: 10.1002/mame.201000078

Keywords: clay; CO_2; flammability; foam extrusion; nanocomposites

[1] D. L. Tomasko, A. Burley, L. Feng, S.-K. Yeh, K. Miyazono, S. Nirmal-Kumar, I. Kusaka, K. W. Koelling, *J. Supercrit. Fluids* **2009**, *47*, 493.
[2] L. J. M. Jacobs, M. F. Kemmere, J. T. F. Keurentjes, *Green Chem.* **2008**, *10*, 731.
[3] K. W. Suh, C. P. Park, M. J. Maurer, M. H. Tusim, R. De Genova, R. Broos, D. P. Sophiea, *Adv. Mater.* **2000**, *12*, 1779.
[4] J. W. S. Lee, C. B. Park, S. G. Kim, *J. Cell. Plast.* **2007**, *43*, 297.
[5] H. Sun, J. E. Mark, S. C. Tan, N. Venkatasubramanian, M. D. Houtz, F. E. Arnold, C. Y.-C. Lee, *Nonlinear Opt. Quantum Opt.* **2004**, *31*, 1.
[6] X. Dai, Z. Liu, Y. Wang, G. Yang, J. Xu, B. Han, *J. Supercrit. Fluids* **2005**, *33*, 259.
[7] K. R. Chynoweth, Z. H. Stachurski, *Polymer* **1986**, *27*, 1912.
[8] A. I. Cooper, *J. Mater. Chem.* **2000**, *10*, 207.
[9] C. Cravo, A. R. C. Duarte, C. M. M. Duarte, *J. Supercrit. Fluids* **2007**, *40*, 194.
[10] L. Urbanczyk, C. Calberg, C. Detrembleur, C. Jérôme, M. Alexandre, *Polymer* **2010**, *51*, 3520.
[11] C. B. Park, D. F. Baldwin, N. P. Suh, *Polym. Eng. Sci.* **1995**, *35*, 432.
[12] H. E. Naguib, C. B. Park, N. Reichelt, *J. Appl. Polym. Sci.* **2004**, *91*, 2661.
[13] E. D. Weil, S. V. Levchik, *J. Fire Sci.* **2007**, *25*, 241.
[14] S. V. Levchik, E. D. Weil, *Polym. Int.* **2008**, *57*, 431.
[15] J. Q. Wang, W. K. Chow, *J. Appl. Polym. Sci.* **2005**, *97*, 366.
[16] J. W. Gilman, *Appl. Clay Sci.* **1999**, *15*, 31.
[17] M. Alexandre, Dubois. Ph, *Mater. Sci. Eng. R* **2000**, *28*, 1.
[18] F. Laoutid, L. Bonnaud, M. Alexandre, J. M. Lopez-Cuesta, Dubois. Ph, *Mater. Sci. Eng. R* **2009**, *63*, 100.
[19] M. Zammarano, J. W. Gilman, R. H. Kramer, R. Harris, T. J. Ohlemiller, J. R. Shields, "Effect of Nanoparticles on Flammability of Flexible Polyurethane Foams", in: *Recent Advances in Flame Retardancy of Polymeric Materials*, Proceedings of 19th BCC Conference, Stamford 2008.
[20] M. Zammarano, R. H. Kramer, R. Harris, T. J. Ohlemiller, J. R. Shields, S. S. Rahatekar, S. Lacerda, J. W. Gilman, *Polym. Adv. Technol.* **2008**, *19*, 588.
[21] X. Han, C. Zeng, J. Lee, K. W. Koelling, D. L. Tomasko, *Polym. Eng. Sci.* **2003**, *43*, 1261.
[22] L. Urbanczyk, S. Bourbigot, C. Calberg, C. Detrembleur, C. Jérôme, F. Boschini, M. Alexandre, *J. Mater. Chem.* **2010**, *20*, 1567.
[23] S. Bourbigot, M. Le Bras, F. Dabrowski, J. W. Gilman, T. Kashiwagi, *Fire Mater.* **2000**, *24*, 201.
[24] A. B. Morgan, *Polym. Adv. Technol.* **2006**, *17*, 206.
[25] W. Zheng, Y. H. Lee, C. B. Park, *J. Cell. Plast.* **2006**, *42*, 271.
[26] Y. H. Lee, K. H. Wang, C. B. Park, M. Sain, *J. Appl. Polym. Sci.* **2007**, *103*, 2129.
[27] X. Han, J. Shen, H. Huang, D. L. Tomasko, J. Lee, *Polym. Eng. Sci.* **2007**, *47*, 103.
[28] M. Sauceau, C. Nikitine, E. Rodier, J. Fages, *J. Supercrit. Fluids* **2007**, *43*, 367.
[29] L. Urbanczyk, C. Calberg, F. Stassin, M. Alexandre, R. Jérôme, C. Jérôme, C. Detrembleur, *Polymer* **2008**, *49*, 3979.
[30] J. W. S. Lee, K. Wang, C. B. Park, *Ind. Eng. Chem. Res.* **2005**, *44*, 92.
[31] M. Mainil, L. Urbanczyk, C. Calberg, A. Germain, C. Jérôme, S. Bourbigot, J. Devaux, M. Sclavons, *Polym. Eng. Sci.* **2010**, *50*, 10.
[32] C. B. Park, A. H. Behravesh, R. D. Venter, *Polym. Eng. Sci.* **1998**, *38*, 1812.
[33] BASF Luran358N Product Data Sheet.
[34] L. Urbanczyk, C. Calberg, S. Benali, S. Bourbigot, E. Espuche, F. Gouanvé, P. Dubois, A. Germain, C. Jérôme, C. Detrembleur, M. Alexandre, *J. Mater. Chem.* **2008**, *18*, 4623.
[35] N. Fedullo, E. Sorlier, M. Sclavons, C. Bailly, J.-M. Lefebvre, J. Devaux, *Prog. Org. Coat.* **2007**, *58*, 87.
[36] P. H. Nam, P. Maiti, M. Okamoto, T. Kotaka, *Polym. Eng. Sci.* **2002**, *42*, 1907.
[37] M. Modesti, A. Lorenzetti, S. Besco, D. Hrelja, S. Semenzato, R. Bertani, R. A. Michelin, *Polym. Degrad. Stab.* **2008**, *93*, 2166.
[38] A. I. Balabanovich, V. P. Prokopovich, *J. Fire Sci.* **2005**, *23*, 417.
[39] M. Le Bras, S. Bourbigot, B. Revel, *J. Mater. Sci.* **2009**, *34*, 5777.

DOI: 10.1002/mame.201000078